

Modulation of Luttinger liquid exponents in multi-walled carbon nanotubes

S. Bellucci^a, J. González^b, P. Onorato^{a,c} and E. Perfetto^{a,b}

^aINFN, Laboratori Nazionali di Frascati, P.O. Box 13, 00044 Frascati, Italy.

^bInstituto de Estructura de la Materia, Consejo Superior de Investigaciones Científicas, Serrano 123, 28006 Madrid, Spain

^cDipartimento di Scienze Fisiche, Università di Roma Tre, Via della Vasca Navale 84, 00146 Roma, Italy

(Dated: September 20, 2018)

We develop in this paper a theoretical framework that applies to the intermediate regime between the Coulomb blockade and the Luttinger liquid behavior in multi-walled carbon nanotubes. Our main goal is to confront the experimental observations of transport properties, under conditions in which the thermal energy is comparable to the spacing between the single-particle levels. For this purpose we have devised a many-body approach to the one-dimensional electron system, incorporating the effects of a discrete spectrum. We show that, in the crossover regime, the tunneling conductance follows a power-law behavior as a function of the temperature, with an exponent that oscillates with the gate voltage as observed in the experiments. Also in agreement with the experimental observations, a distinctive feature of our approach is the existence of an inflection point in the log-log plots of the conductance vs temperature, at gate voltages corresponding to peaks in the oscillation of the exponent. Moreover, we evaluate the effects of a transverse magnetic field on the transport properties of the multi-walled nanotubes. For fields of the order of 4 T, we find changes in the band structure that may be already significant for the outer shells, leading to an appreciable variation in the power-law behavior of the conductance. We then foresee the appearance of sensible modulations in the exponent of the conductance for higher magnetic fields, as the different subbands are shifted towards the development of flat Landau levels.

PACS numbers: 73.63.Fg, 73.22.-f, 73.23.-b

I. INTRODUCTION

Recent progresses in nanotechnology has revealed many novel transport phenomena in mesoscopic low-dimensional structures. Carbon nanotubes (CNs) were discovered by Iijima in 1991¹, as a by-product of carbon fullerene production. Thus, since then, a new field of research in mesoscopic physics has opened². CNs are basically rolled up sheets of graphite (hexagonal networks of carbon atoms) forming tubes that are only nanometers in diameter. The electronic properties of CNs depend on their diameter and chiral angle (helicity) parameterized by a roll-up (wrapping) vector (n, m) ³. Hence it follows that some nanotubes are metallic with high electrical conductivity, while others are semiconducting with relatively low band gaps. They may also display different electronic properties depending on whether they are single-walled carbon nanotubes (SWNTs) or multi-walled carbon nanotubes (MWNTs). MWNTs are typically made of several (typically 10) concentrically arranged graphene sheets with a radius of about 5 nm and lengths in the range of 1 – 100 μm .

Several electrical transport experiments have been done by using CNs. In these experiments the effects of the Coulomb interaction are quite relevant, and the way they manifest depend mainly on the size of the system, the temperature, and the quality of the contacts used in experiments. Thus, MWNTs show for instance different transport regimes from ballistic transport (conductance quantization^{4,5}, Luttinger liquid-like^{6,7}) to diffusive transport⁸ and also strong localization^{9,10}.

When the contacts are not highly transparent, the measurements of the conductance and the differential

conductivity reflect the strong Coulomb repulsion in CNs^{11,12}. At low temperature, $T \lesssim 1$ K, the zero-bias conductance is strongly influenced by quantum mechanical effects and shows regular oscillations corresponding to the so-called *single electron tunneling* (SET), because it arises from the electrons going one at a time through the device^{13,14}. The voltage between two peaks is determined by the energy for adding an electron to the device between the potential barriers. This addition energy depends on the level spacing, due to the momentum quantization, and on the electron-electron interaction¹⁵. This is the Coulomb blockade (CB) regime where the tunneling transparency of a barrier vanishes owing to the electron-electron interaction. The differential conductivity of individual MWNTs has been measured in Ref. 16, where CB and energy level quantization have been observed.

When the temperature increases, so that the thermal energy is much larger than the level spacing, the transport measurements reflect instead the many-body properties of the system. In fact, the electron-electron interaction in a one-dimensional (1D) system is expected to lead to the formation of a Luttinger liquid (LL) with properties very different from those of the non-interacting Fermi gas¹⁷. The LL state is characteristic of 1D clean (ballistic) conductors, which have unusual electronic properties that cannot be explained by Fermi liquid theory.

Landau quasiparticles are unstable in 1D systems of interacting electrons, in which the low-energy excitations take the form of plasmons (collective electron-hole pair modes) that are the stable excitations: this is known as the breakdown of Fermi liquid in 1D^{18,19,20}. The LL state has two main features:

- i) the power-law dependence of physical quantities,

such as the tunneling density of states (TDOS), as a function of energy or temperature;

ii) the spin-charge separation: an additional electron in the LL decays into decoupled spin and charge wave packets, with different velocities for charge and spin.

Characteristic experimental signatures support the assumed LL behaviour of CNs^{21,22,23,24}. In fact the power-law dependence of physical observables follows from the behavior of the TDOS as a function of the energy or the temperature: the tunneling conductance G reflects the power law dependence of the TDOS in a small-bias experiment²⁵

$$G = dI/dV \propto T^\alpha \quad (1)$$

for $eV_b \ll k_B T$, V_b being bias voltage. Such kind of signatures of LL behavior have been observed in single-walled as well as in multi-walled nanotubes. In MWNTs the observed values of α lie between 0.04 and 0.3, and results in agreement with the experimental values have been obtained in previous theoretical works^{26,27,28,29}.

In this paper we introduce a theoretical description of the crossover as the temperature decreases from the LL regime to the CB regime. We do this in order to confront the experimental data reported in a recent letter by Kanda *et al.*³⁰, in which the intermediate regime has been explored measuring the zero-bias conductance at temperatures where the thermal energy becomes comparable to the level spacing in the discrete single-particle spectrum. In Ref. 30 the authors have reported a systematic study of the gate voltage dependence of the LL-like behaviour in MWNTs, showing the dependence of the exponent α on gate voltage, with values of α ranging from 0.05 to 0.35. The main results of Ref. 30 are as follows:

i) the gate-voltage (V_g) dependence of the exponent α below 30 K exhibits periodic oscillations; the characteristic V_g scale for α variation, ΔV_g , is around 1V;

ii) changes in the exponent α are observed in the plots of the conductance at an inflection temperature $T^* \sim 30$ K, for values of V_g corresponding to peaks of α .

iii) the exponent α depends significantly on the transverse magnetic field acting on the CN. α is reduced from a value of 0.34, at a peak in the α oscillations, to a value 0.11, for a magnetic field $B = 4$ T. In most cases, the exponent α becomes smaller for higher magnetic fields.

In their letter, Kanda *et al.* do not find plausible the explanation of the mentioned features starting from a LL description of the MWNTs. In this respect, Egger has considered in Ref. 31 a model for MWNTs composed of a number N_{SH} of ballistic metallic shells. The author has discussed there a low-energy theory for the MWNTs including long-ranged Coulomb interactions and internal screening effects. The theory may be also extended to include the effect of a variable number of conducting modes modulated by the doping level. However, Kanda *et al.* rule out the possibility that the change in the number of subbands at the Fermi level may be at the origin of the features observed in their experiment, as long as the

subband spacing is too large to be consistent with the period of the oscillations.

Then, Kanda *et al.* turn to a different kind of theory that considers the MWNT as a diffusive conductor. Egger and Gogolin³² have calculated the TDOS of doped MWNTs including disorder (with mean free path l smaller than the radius R) and electron-electron interactions. MWNTs may display an effective and nonconventional CB arising from tunneling into a strongly interacting disordered metal, leading to LL-like zero-bias anomalies: the exponent becomes $\alpha = (R/2\pi\hbar D\nu_0) \log(1 + \nu_0 U)$, where D is the diffusion constant, $\nu_0 = N_s/2\pi\hbar v_F$ is the noninteracting density of states depending on the number of subbands N_s and the Fermi velocity v_F , and U_0 is an effectively short-ranged 1D interaction. Substituting these parameters by pertinent values yields an estimate $\alpha \simeq R/N_s l$, that is near the experimentally observed values.

Kanda and coworkers conclude that this second theory better explains the experimental results, by assuming that the mean-free path l may fluctuate with the gate voltage. This is based on the theoretical work by Choi *et al.*³³, that have studied the effects of single defects on the local density of states via resonant backscattering. However, the argument of Kanda *et al.* has not addressed the question of how a random distribution of defects may produce the oscillations observed in the experiment. We believe otherwise that the dependence of the α exponent on the gate voltage is in correspondence with a definite periodic structure of the single-particle density of states.

In the next section, we put forward the idea that there exists a clear relation between the periodic oscillations in the α exponent and the quantization of the energy levels in the MWNTs³⁴. Building on this idea, in section III we introduce an energy distribution function which takes into account the effects of the quantization at low temperature and can be compared with the Fermi-Dirac distribution in the limit of high temperature. Next, in section IV we develop a theoretical approach based on many-body theory, in order to deal with the low-energy effects of the the long-range Coulomb interaction in the 1D electron system. We introduce in that scheme the discussed energy distribution function, for the sake of evaluating the effects of the discrete spectrum on the exponent α . The results of this approach are reported in section V, where we carry out the comparison between our theoretical predictions and the experiments. The effects of a transverse magnetic field are considered in section VI. In section VII we highlight how the distinctive features of our approach match naturally with the experimental observations, and we close with some concluding remarks and perspectives in section VIII.

II. ANALYSIS OF THE EXPERIMENTAL OSCILLATIONS

Here we discuss the values of relevant parameters, in order to compare later the experimental results with the theoretical predictions.

The transverse quantization energy of the nanotube, which corresponds to the distance between two nearest subbands, is given by $\Delta E_{\perp} \approx \hbar v_F/R$, where the Fermi velocity is $v_F = 8 \times 10^5$ m/s and we take a nanotube radius $R \approx 5$ nm. On the other hand, the longitudinal quantization energy reads $\Delta \varepsilon_L = \hbar v_F/L$, where in the experiments $L \approx 4 \div 6 \mu\text{m}$ (here we are considering the entire length of the MWNT, $L \approx 5.7(4.7) \mu\text{m}$, rather than the length of its portion between the electrodes, $d \approx 0.7(1.0) \mu\text{m}$). The ratio turns out to be $\frac{\Delta E_{\perp}}{\Delta \varepsilon_L} \approx \frac{L}{2\pi R} \approx 10 \div 100$.

In comparing the theoretical estimates with the experiment, there appears a conversion factor given by the coupling constant γ between the gate electrode and the MWNT. This factor is approximately $\gamma = C/C_0$, where C is the capacitance between the metal electrodes and the MWNT while C_0 is the capacitance between the gate electrode and the MWNT. In the experiments by Kanda *et al.*^{30,35} $C \approx 1\text{fF}$ and $C_0 \approx 1\text{aF}$ so that we obtain $\gamma \approx 1 \times 10^3$.

Using these parameters Kanda and coworkers confute the above mentioned model based on the LL theory. In fact, the transverse quantization energy is about 0.1 eV, so that the typical value $\Delta V_g = \gamma \Delta E_{\perp}$ for the change in the number of subbands N_s at the Fermi level is about 10^2V . This value is much larger than the period for the gate voltage in the observed oscillations, which corresponds to some Volts. This theory would also predict a stepwise change in α as a function of V_g , which is not in agreement with the oscillatory behavior measured.

In the experiment, the measured value of the period ΔV_g is around 3 V at a temperature T below 30 K. As shown by the cited authors in a previous paper³⁵, where they reported the observation of the CB effect in MWNT, a similar value of ΔV_g corresponds to a period (a sequence of 4 peaks or diamonds) in the zero bias conductance at very low temperature $T \sim 30$ mK.

Following the usual formalism¹⁵ we can calculate the period as $\Delta V_g = \gamma(v_F \hbar/L + 4U)$ ¹⁶. If we neglect the electron-electron interaction U , we can assume $\Delta V_g \sim \gamma v_F \hbar/L$, in order to compare the number of oscillations in a definite range of the gate voltage (-10V to 10V in the experiment) observed for two different nanotubes (i.e. samples A and B in Fig. 1, respectively). Thus, we expect that the number of oscillations depends on the length as

$$\frac{n_A}{n_B} = \frac{L_A}{L_B} = \frac{5.7\mu\text{m}}{4.7\mu\text{m}} \approx 1.2.$$

From the experimental data (see Fig. 1) we observe respectively 10 and 8 oscillations, corresponding to an en-

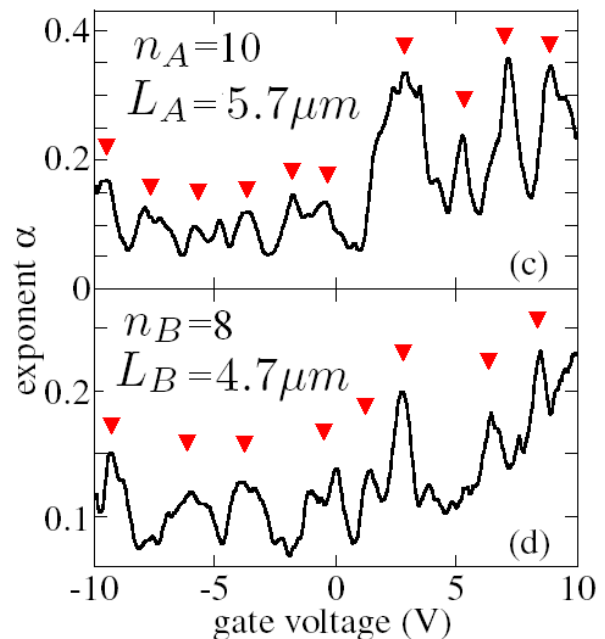


FIG. 1: A figure summarizing the gate-voltage dependence of α in sample A ($L_A = 5.7\mu\text{m}$ top) of Ref. 30, calculated from the data below 30°K . A similar $\alpha - V_g$ plot is obtained for sample B ($L_A = 4.7\mu\text{m}$ bottom).

ergy spacing $\Delta \varepsilon \approx 2 \div 2.5$ meV, in perfect agreement with our estimate. This agreement suggests a theory based on a microscopic description of the single-particle spectrum, in order to explain the oscillations. Here the quantized energy levels play a central role. This theory has to be valid in the intermediate regime between very low temperature, where the peaks of the CB are measured by increasing V_g , and room temperature, where the LL behaviour prevails. To this aim, we will rely on the 1D many-body approach, incorporating at the same time the discrete character of the spectrum which arises from the finite geometry of the system.

III. SINGLE-PARTICLE PROPERTIES

In the introduction of microscopic features in the many-body formalism, a central role is played by the energy distribution function (EDF) $n(\varepsilon; \varepsilon_F)$. In the many-body approach to electron liquids, the function $n(\varepsilon, \varepsilon_F)$ corresponds to the Fermi-Dirac distribution, which is usually replaced by the Heaviside step function $\vartheta(\varepsilon - \varepsilon_F)$ in order to simplify the calculations.

At very low temperatures, as the ones that are needed for the CB regime, the EDF has to reflect the discreteness of the energy levels. Thus, some pattern of peaks, corresponding to the quantized energy levels, has to be present. Hence, at low temperatures, where the microscopic level quantization is manifest, peaks arise with a shape smoothed by the growth of the temperature. The

spacing $\Delta\varepsilon$ of the peaks depends on the nanotube length L

$$\Delta\varepsilon = \frac{v_F h}{L},$$

This value yields a temperature $T_c \approx \Delta\varepsilon/k_B$, above which we expect that the oscillations will be smoothed.

The thermal energy $k_B T_c$ governs then the crossover between two different regimes. From our analysis, it is clear that two scales for the behavior as a function of temperature characterize the system, corresponding to the longitudinal and the transverse quantization energies, although the second one turns out to be about $10 \div 100$ times larger than $k_B T_c$.

We can model the n -th peak of the EDF by a normalized function $f(\varepsilon, n)$, with a dependence on temperature consistent with the line shape for a thermally broadened resonance³⁶

$$f(\varepsilon, n) = \frac{1}{4kT \cosh^2\left(\frac{\varepsilon - n\Delta\varepsilon}{2kT}\right)}, \quad (2)$$

where $n\Delta\varepsilon$ stands for the position of the n -th energy level. The energy distribution function is cutoff by the Fermi energy ε_F , as it is given by

$$n(\varepsilon; \varepsilon_F) = \sum_{n=0}^{\infty} f(\varepsilon, n) \theta(\varepsilon_F - \varepsilon). \quad (3)$$

Alternatively we could introduce a smooth cutoff at the Fermi energy, taking into account thermal effects

$$n(\varepsilon; \varepsilon_F) = \sum_{n=0}^{\infty} f(\varepsilon, n) \frac{1}{1 + e^{(\varepsilon - \varepsilon_F)/kT}}. \quad (4)$$

Anyway the sharp cutoff given by $\theta(\varepsilon_F - \varepsilon)$ is more convenient, in order to proceed with analytical computations. On the other hand, we have checked that the presence of the smooth cutoff does not change appreciably the whole scenario.

At high temperatures, we can neglect the level spacing and calculate the EDF by integrating

$$\begin{aligned} n(\varepsilon; \varepsilon_F) &\approx \int_{-\infty}^{\varepsilon_F/\Delta\varepsilon - 1/2} dy f(\varepsilon, y) \\ &= \frac{1}{1 + e^{(\varepsilon - \varepsilon_F + \Delta\varepsilon/2)/kT}}. \end{aligned} \quad (5)$$

The latter formula gives the Fermi-Dirac distribution, which is usually approximated with the step function. However, the energy distribution function has in general a more structured shape, that depends on the ratio between the level spacing $\Delta\varepsilon$ and the thermal energy kT as illustrated in Fig. 1.

The structure of peaks in the energy distribution function affects several objects in the many-body theory, like the one-loop polarization $\Pi^{(0)}(q, \omega_q)$. This object counts the number of particle-hole excitations that can be built

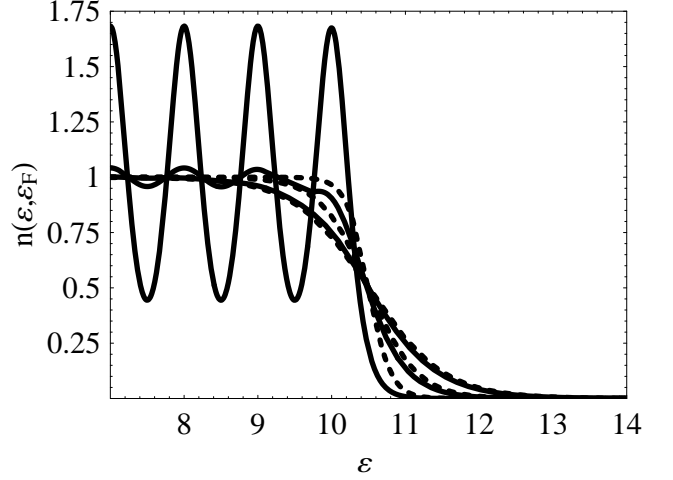


FIG. 2: Plot of the energy distribution function $n(\varepsilon; \varepsilon_F)$ for different values of the temperature corresponding to $kT/\Delta\varepsilon = 0.25, 0.6, 1.0$. The solid lines have been obtained from Eq. (3) and the dashed lines by using the Fermi-Dirac distribution (5).

with momentum q across the Fermi level. Thus, in the case of a model with linear dispersion $\varepsilon(k) \approx v_F k$, it becomes proportional at zero temperature to

$$\begin{aligned} &\int_{-\infty}^{\infty} \frac{dk}{2\pi} \frac{\theta(q+k-k_F) - \theta(k-k_F)}{v_F q} \\ &= \frac{1}{v_F q} \int_0^q \frac{dk}{2\pi} = \frac{1}{2\pi v_F}. \end{aligned} \quad (6)$$

In the approach based on the distribution function given by (3), the peaks give rise to a factor in the integration that reflects the discrete structure. Therefore Eq.(6) becomes

$$\begin{aligned} &\int_{-\infty}^{\infty} \frac{dk}{2\pi} \Delta\varepsilon \frac{n(v_F(q+k); \varepsilon_F) - n(v_F k; \varepsilon_F)}{v_F q} \\ &= \frac{1}{v_F q} \int_0^q \frac{dk}{2\pi} \Delta\varepsilon \sum_{n=0}^{\infty} f(v_F k, n) \approx \frac{1}{2\pi v_F} N_T(\varepsilon_F), \end{aligned} \quad (7)$$

where at first order the function $N_T(\varepsilon_F)$ can be taken independent on q . Given the sharp cutoff, the N_T function gets a simple form:

$$\begin{aligned} &\int_0^q dk \Delta\varepsilon \sum_{n=0}^{\infty} f(v_F k, n) = \\ &\frac{\Delta\varepsilon}{2v_F} \sum_{n=0}^{\infty} \left[\tanh\left(\frac{\varepsilon_F + v_F q - n\Delta\varepsilon}{2kT}\right) - \tanh\left(\frac{\varepsilon_F - n\Delta\varepsilon}{2kT}\right) \right] \\ &\approx q \frac{\Delta\varepsilon}{4kT} \sum_{n=0}^{\infty} \left[1 - \tanh^2\left(\frac{\varepsilon_F - n\Delta\varepsilon}{2kT}\right) \right] = q N_T(\varepsilon_F). \end{aligned} \quad (8)$$

Therefore it holds

$$N_T(\varepsilon_F) = \frac{\Delta\varepsilon}{4kT} \sum_{n=0}^{\infty} \left[1 - \tanh^2\left(\frac{\varepsilon_F - n\Delta\varepsilon}{2kT}\right) \right]. \quad (9)$$

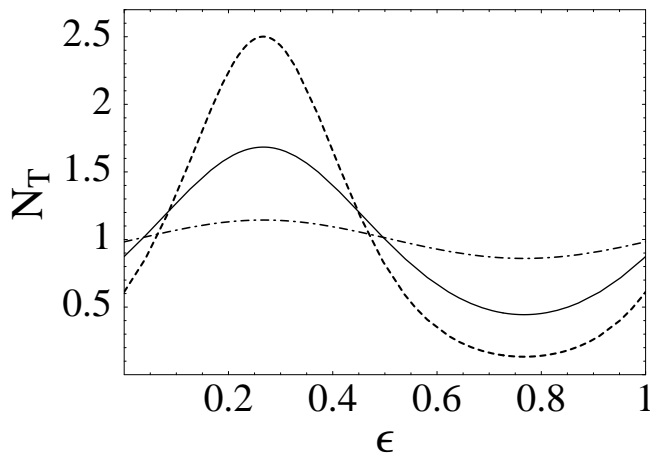


FIG. 3: Plot of $N_T(\varepsilon_F)$ for three different values of $kT/\Delta\varepsilon$: $kT/\Delta\varepsilon = 0.1$ (dashed), $=0.15$ (solid), $=0.3$ (dotted-dashed). ε is in unit of $\Delta\varepsilon$

This function is represented in Fig. 3. As expected, $N_T(\varepsilon)$ is periodic with period $\Delta\varepsilon$.

We introduced the function N_T depending on the Fermi energy ε_F . In this respect, the position of ε_F , tunable by the gate voltage V_g , fixes the portion of the last peak that we have to integrate. It is clear that, from an experimental point of view, ε_F is in correspondence with the value of the gate voltage V_g , so that it can be shifted in a continuous way, allowing for the exploration of the region between two peaks in Fig. 2.

IV. MANY-BODY APPROACH

In the CNs, the relevant interaction is given by the large Coulomb potential at small momentum-

transfer^{37,38}. It is known that the Coulomb interaction remains long-ranged in a 1D electron system^{26,39}, and this property is also shared by the graphene sheet, which has a vanishing 2D density of states at the Fermi level. To obtain a sensible expression of the 1D interaction, we may start from the representation of the $1/|\mathbf{r}|$ Coulomb potential in three spatial dimensions as the Fourier transform of the propagator $1/\mathbf{k}^2$

$$\frac{1}{|\mathbf{r}|} = \int \frac{d^3k}{(2\pi)^3} e^{i\mathbf{k}\cdot\mathbf{r}} \frac{1}{\mathbf{k}^2} \quad (10)$$

If the interaction is projected onto one spatial dimension, by integrating for instance the modes in the transverse dimensions, then the Fourier transform has the usual logarithmic dependence on the longitudinal momentum²⁶

$$\frac{1}{|x|} \approx - \int \frac{dk}{2\pi} e^{ikx} \frac{1}{2\pi} \log(k) \quad (11)$$

In our case, the scale of the longitudinal momentum k in the logarithm is dictated by the existence of a short-distance cutoff k_c , from the small transverse size of the electron system. Thus, we end up with a representation of the Fourier transform $\tilde{V}(k)$ of the 1D Coulomb potential

$$\tilde{V}(k) \approx \frac{1}{2\pi} \log(k_c/k) \quad (12)$$

where $k_c \sim 1/R$.

Our interest focuses in describing the interaction among a number N_s of subbands crossing the Fermi level in the conducting shell of a multi-walled nanotube. Thus, we write the hamiltonian for the electron fields $\Psi_{\pm a\sigma}$ encoding the modes of the different branches with linear dispersion about the Fermi points $p_{Fa}, -p_{Fa}$:

$$H = \int_{-k_c}^{k_c} dp \sum_{a=1}^{N_s} \psi_{\pm a\sigma}^\dagger(p) (\pm v_F p) \psi_{\pm a\sigma}(p) + e^2 \int_{-k_c}^{k_c} dp \rho(p) \tilde{V}(p) \rho(-p) \quad (13)$$

In the above expression, $\rho(p)$ stands for the charge density made from the sum of all the electron densities for the fields $\psi_{\pm a\sigma}(p)$.

In the hamiltonian (13), we have neglected interactions that lead to a change of chirality (\pm) of the fields, as they imply a large momentum-transfer of the order of $2k_F$ and are therefore subdominant with respect to the large Coulomb interaction at small momentum-transfer. Those so-called backscattering interactions are known to remain negligible down to extremely low energies. On the other hand, the model build from interactions between currents with well-defined chirality has some inter-

esting properties. One of them is that, when performing the perturbative calculation of the polarization function $\Pi(q, \omega_q)$, the self-energy corrections cancel order by order against the vertex corrections. Thus, the exact result is just given by the bare polarization function. In our case, upon the introduction of the different subbands and the mentioned effects in the single-particle density of states, we have

$$\Pi(q, \omega_q) = \frac{2}{\pi} N_s N_T(\varepsilon_F) \frac{v_F q^2}{\omega_q^2 - v_F^2 q^2} \quad (14)$$

Moreover, there is further simplification of the dia-

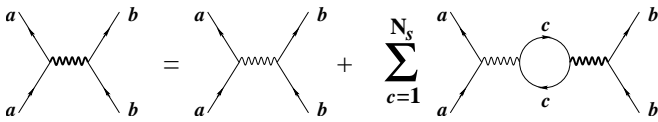


FIG. 4: Self-consistent diagrammatic equation for the dressed Coulomb interaction.

grammatics from the fact that all the fermion loops with more than two interaction lines vanish identically in 1D. Thus, the dressed Coulomb interaction has to satisfy the self-consistent equation shown in Fig. 4, that amounts to the RPA sum of particle-hole contributions.

We are mainly interested in obtaining the quasiparticle properties in the model governed by (13), which requires the computation of the electron self-energy $\Sigma(q, \omega_q)$. As long as the RPA provides the exact expression of the dressed Coulomb interaction, a sensible representation of the self-energy is given by the partial sum of the perturbative expansion shown in Fig. 5. Correspondingly, we may express the electron self-energy in the form

$$\Sigma(k, \omega_k) = i \int_{-k_c}^{k_c} \frac{dq}{2\pi} \int_{-\infty}^{\infty} \frac{d\omega_q}{2\pi} G^{(0)}(k-q, \omega_k - \omega_q) \times \frac{\tilde{V}(q)}{1 - \tilde{V}(q)\Pi(q, \omega_q)}, \quad (15)$$

where $G^{(0)}(k, \omega_k)$ stands for the free electron propagator. For the evaluation of the scaling properties of the quasiparticle parameters, it is enough to obtain the logarithmic dependence of the function $\Sigma(q, \omega_q)$ on the high-energy cutoff $E_c \sim v_F k_c$. Thus, the representation in Fig. 5 misses corrections to the fermion line $G^{(0)}$ as well as corrections to the three-point vertex at the end of the line, but these do not introduce new divergences in the cutoff E_c and can be safely disregarded in the determination of the electron field scale.

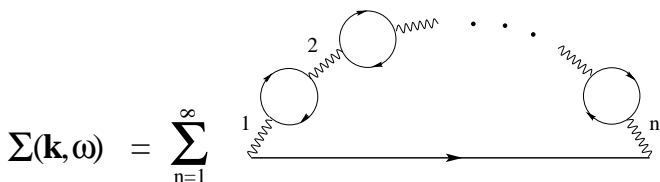


FIG. 5: Set of diagrams for the computation of the electron self-energy, where each particle-hole bubble represents the full polarization operator.

We therefore concentrate on the computation of the contributions that diverge with the cutoff E_c in (15). Order by order in perturbation theory, we find that the same kind of logarithmic dependence appears in the linear terms proportional to k and ω_k . We can recast the whole perturbative series into the expression

$$\Sigma(k, \omega_k) \approx \frac{1}{2\pi^{3/2}} \frac{\tilde{V}(q_0)e^2}{v_F} \sum_{n=0}^{\infty} (-1)^n g^n \frac{n\Gamma(n+1/2)}{(n+1)!}$$

$$\begin{aligned} & \times (\omega_k \pm v_F k) \log(E_c) \quad (16) \\ & = -\frac{1}{4N_s N_T} \left(\sqrt{1+g} + \frac{1}{\sqrt{1+g}} - 2 \right) \\ & \times (\omega_k \pm v_F k) \log(E_c) \quad (17) \end{aligned}$$

where the effective coupling is given by $g = 2N_s N_T \tilde{V}(q_0) e^2 / \pi v_F$, in terms of a suitable average momentum q_0 ⁴⁰.

The frequency and momentum-dependence in Eq. (17) shows that such self-energy corrections represent a renormalization of the electron field operator. Then it is convenient to define a renormalized electron field Ψ_R related in each case to the bare electron field Ψ through a scale factor $Z^{1/2}(E_c)$:

$$\Psi_R = Z^{1/2}(E_c) \Psi \quad (18)$$

The renormalization factor $Z(E_c)$ must be fixed so that it makes finite the renormalized electron Green function $G(k, \omega_k)$. This is given by

$$\begin{aligned} \frac{1}{G} &= \frac{1}{G^{(0)}} - \Sigma(k, \omega_k) \\ &\approx Z^{-1}(E_c) (\omega_k \pm v_F k) \\ &\quad + Z^{-1}(E_c) (\omega_k \pm v_F k) \alpha(g) \log(E_c) \quad (19) \end{aligned}$$

where

$$\alpha(g) = \frac{1}{4N_s N_T} \left(\sqrt{1+g} + \frac{1}{\sqrt{1+g}} - 2 \right) \quad (20)$$

The requirement of cutoff-independence of the electron Green function leads to absorb the logarithmic dependence on E_c into the renormalization factor $Z(E_c)$. Thus we get the scaling equation

$$E_c \frac{d}{dE_c} \log Z(E_c) = \alpha(g). \quad (21)$$

We observe that $Z(E_c)$ follows a power-law behavior as a function of the energy cutoff E_c . We may identify the factor $Z(E_c)$ with the weight of the electron quasiparticles, which vanishes as the Fermi level is approached in the limit $E_c \rightarrow 0$. We capture in this way one of the most genuine features of the many-body theory in 1D, namely the absence of low-energy excitations with fermionic character, which defines the Luttinger liquid class of 1D electron liquids.

V. TUNNELING DENSITY OF STATES

The power-law behavior of the quasiparticle weight $Z(E_c)$ translates into a similar dependence on energy of the tunneling density of states $n(\varepsilon)$. By trading the dependence on the high-energy cutoff by the energy measured with respect to the Fermi level, we obtain the scaling behavior

$$n(\varepsilon) \sim N_s Z(\varepsilon) \sim \varepsilon^{\alpha(g)} \quad (22)$$

Usually the behavior of the TDOS is obtained by measuring its dependence on temperature or bias voltage. The exponent in (22) is then to be compared with the measurements of power-law behavior observed in the plots of conductance versus temperature, or in the differential conductivity.

Regarding the experiments in Ref. 30, we are in disposition to explain the oscillations observed in the exponent of the conductance, in a temperature regime corresponding to a thermal energy of the order of the level spacing $\Delta\varepsilon$. The point is that, as we shift the Fermi level along the structure of single-particle peaks in the spectrum, the α exponent has to reflect the modulation of the periodic factor $N_T(\varepsilon)$. As mentioned before, the period of the oscillations is in agreement with the change in gate voltage required for a shift $\Delta\varepsilon$ of the Fermi level. We comment now on several features regarding the amplitude of the oscillations.

It becomes very convenient to plot the expression of the exponent $\alpha(g)$ as a function of the variable $N_s N_T$. This depends also on the effective coupling $\tilde{V}(q_0)e^2/v_F$ of the Coulomb interaction. We have estimated this quantity by using a value of q_0 consistent with the nanotube length, and taking into account the screening of the interaction, mainly by other shells in the nanotube. Thus, sensible values of $\tilde{V}(q_0)e^2/v_F$ turn out to be of the order of ~ 10 . The exponent α has been represented in Fig. 6 as a function of $N_s N_T$, for two different choices of the effective coupling. We may assume the typical situation in which the MWNTs are hole-doped, with a number of subbands crossing the Fermi level $N_s \approx 6 - 10^{41}$. We observe that, for such an estimate of N_s , the modulation of the N_T factor (with the amplitude reported in section III) accounts for oscillations of α reaching values as high as ≈ 0.3 (for a large value of the effective coupling) and as low as ≈ 0.05 (for a small value of g and a large number of subbands).

It is actually quite plausible that the drift observed in general in the average value of the α exponent (towards larger values for higher gate voltages) may be the consequence of a change in the Fermi velocity as the Fermi level approaches the top of the lowest partially filled subband. We note that the height reached by the oscillations in the α exponent is different in the two plots of experimental measures shown in Figs. 2(c) and 2(d) in Ref. 30. This may be attributed to a different relative position of the Fermi level between two consecutive subbands in the nanotube bandstructure. We have modeled the proximity to the point with divergent density of states at the top ε_T of a given subband by allowing for a dependence of the Fermi velocity $v_F(\varepsilon_F) \sim \sqrt{\varepsilon_T - \varepsilon_F}$. When this is taken into account in conjunction with the modulation of the periodic function $N_T(\varepsilon_F)$, we obtain a picture for the dependence of the α exponent on gate voltage which is in good qualitative agreement with the oscillations reported in Ref. 30, as shown in Fig. 7.

We observe the similarity of the plot in Fig. 7 with the experimental curves in Fig. 1 for the exponent over

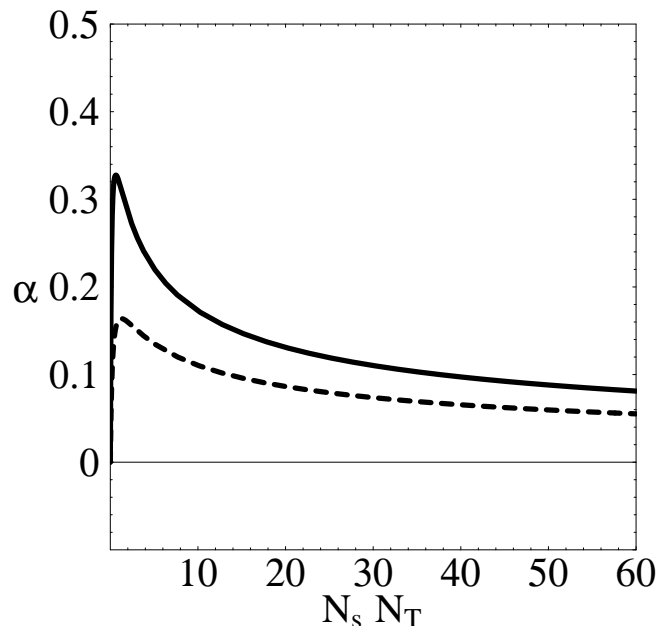


FIG. 6: Plot of the exponent α as a function of the product of the number of subbands N_s and the weight N_T in the single-particle spectrum.

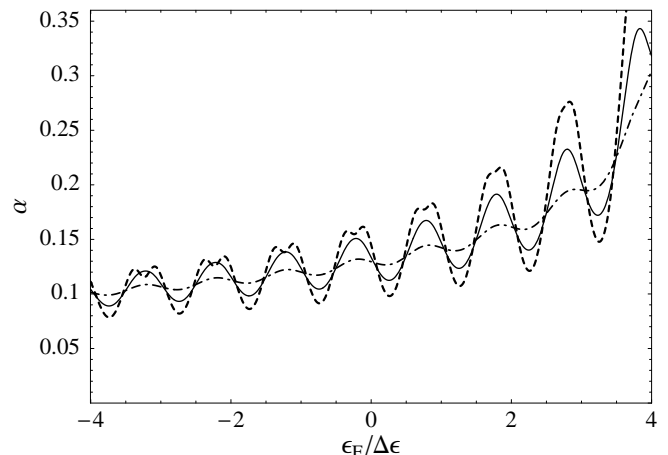


FIG. 7: Plot of the exponent α as a function of the Fermi energy ε_F (in units of $\Delta\varepsilon$) for different values of temperature $kT/\Delta\varepsilon = 0.1$ (dashed), 0.15 (solid), 0.3 (dotted-dashed).

the 20 V range in the gate voltage. The oscillations are significant for low values of the thermal energy $k_B T$, as compared to $\Delta\varepsilon$. For higher temperatures the thermal fluctuations erase the structure of superposed peaks in (3), what leads in turn to the disappearance of the oscillations in the α exponent.

An important point reinforcing the above interpretation of the experimental measures is that the dependence on the variable $N_s N_T(\varepsilon_F)$ shown in Fig. 6 translates naturally into an asymmetric behavior of the exponent α , when the oscillations approach the peak of

the curve near $\alpha \approx 0.3$. If we consider for instance a doped nanotube with $N_s = 10$ and an effective coupling $\tilde{V}(q_0)e^2/v_F \approx 12$, we observe that the exponent may run from a value $\alpha \approx 0.18$ for $N_T = 1$ to a value $\alpha \approx 0.3$ for reasonably small N_T . However, it is clear that the other side of the oscillation does not have the same magnitude. This is consistent with the fact that inflection points in the plots of the conductance versus temperature have been observed for peak values in the exponent oscillations. In our model, the values corresponding to a dip for $N_T > 1$ do not deviate much from the high-temperature behavior recovered for $N_T \approx 1$. It is also remarkable that the inflection points have been found experimentally to correspond to the highest oscillations for large gate voltage. Again, this is consistent with our theoretical interpretation, in which the lower values of the exponent α correspond to smaller values of the effective coupling that do not support large variations upon changes in N_T , as shown from the lower curve in Fig. 6.

VI. MAGNETIC FIELD EFFECTS

The experiments reported in Ref. 30 have also shown that the exponent in the power-law behavior of the zero-bias conductance may depend on the applied transverse magnetic field. The magnetic length $l = \sqrt{c/eB}$ corresponding to the field strength used in the experiments ($B = 4$ T) is anyhow larger than the radius of the outer shells in the MWNTs. Then, the resulting band structure must be far from the development of Landau levels, although it must already lead to the features producing the variation observed in the α exponent.

To study the influence of the magnetic field, we have analyzed the change that it may produce in the band structure of nanotubes with different chiralities. Previous investigations have addressed the formation of Landau subbands in carbon nanotubes upon application of a transverse magnetic field. Here we have undertaken a similar computational approach, but applied to nanotubes of large radius $R \sim 10$ nm, corresponding to active shells in multi-walled nanotubes. We have thus resorted to a tight-binding calculation of the hamiltonian in the carbon lattice, with the usual prescription of correcting the transfer integral by appropriate phase factors

$$\exp\left(i\frac{e}{c}\int_{\mathbf{r}}^{\mathbf{r}'}\mathbf{A}\cdot d\mathbf{l}\right) \quad (23)$$

depending on the vector potential \mathbf{A} between nearest-neighbor sites \mathbf{r} and \mathbf{r}' . The vector potential has been chosen in particular with the appropriate functional dependence at the nanotube surface, as described in Ref. 42.

The results of the numerical diagonalization of the tight-binding hamiltonian for a magnetic field $B = 4$ T are shown in Fig. 8. The band structure corresponds to the particular case of a zig-zag nanotube, but it is quite

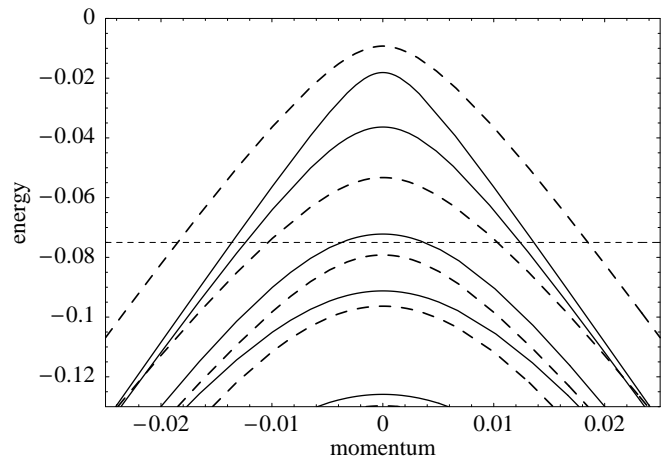


FIG. 8: Energy dispersion relation of a (280,0) zig-zag nanotube with $B = 0$ (solid lines) and $B = 4$ T (dashed lines). The position of the Fermi level for a hole-doped nanotube is also indicated. Energy is in eV (we used a hopping parameter $t = 2.5$ eV between nearest neighbor carbon atoms) and momentum is in \AA^{-1} .

representative of the changes produced in chiral nanotubes upon application of the magnetic field. There is an incipient tendency of the subbands to flatten, an effect which is precursor of the formation of Landau subbands at much higher magnetic field. The two low-energy subbands spanning the gap for semiconducting nanotubes tend to approach, as the lowest Landau level is always at zero energy in the carbon nanotubes. The next subbands move in the opposite direction, towards a very slow reaccommodation along the direction of the higher Landau levels.

In this perspective, there is a significant modification in the low-energy spectrum whenever the number of subbands crossing the Fermi level changes, as a consequence of switching on the magnetic field. This happens in particular when the Fermi level for $B = 0$ is slightly below the top of one of the subbands which is pushed downwards under the action of the magnetic field. Recalling the discussion of the preceding section, this is the instance that corresponds to the higher gate voltages in Fig. 7, where the value of the exponent $\alpha \approx 0.3$ is approached. In these circumstances, a couple of degenerate subbands with large density of states are lost at the Fermi level upon application of the magnetic field. Although the number N_s of subbands contributing to the conduction decreases, the main effect influencing the computation of the exponent α comes from the larger value of v_F in the remaining (outer) degenerate subbands. Taking a value of the Fermi velocity in correspondence with the Fermi level shown in Fig. 8, we find that the exponent is reduced down to a value $\alpha \approx 0.1$, in agreement with the experimental observation reported in Ref. 30.

Although no measures have been reported over a given range of gate voltage in the presence of magnetic field, it is very instructive to apply Eq. (20) to find the results

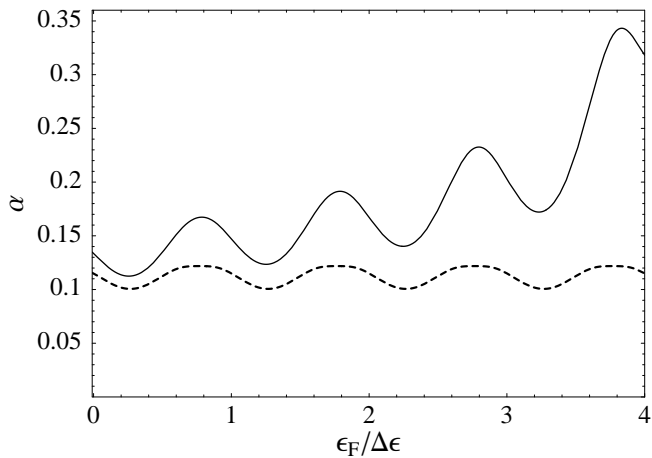


FIG. 9: Plot of the exponent α as a function of the Fermi energy ε_F (in units of $\Delta\varepsilon$) for $B = 0$ (solid line) and $B = 4\text{T}$ (dashed line). Here the temperature is $k_B T / \Delta\varepsilon = 0.15$.

from the change in the band structure shown in Fig. 8. The gate-voltage dependence obtained in this way for the α exponent at $B = 4\text{ T}$ is represented in Fig. 9. We observe that the plot of the exponent is now below the curve corresponding to the oscillations at $B = 0$, which is in agreement with the general statement made in Ref. 30. However, the comparison with the experimental observation reported at a dip in the oscillations ($\alpha \approx 0.06$ at zero magnetic field) shows that our prediction falls short to account for the measured reduction. The experimental result reported at $B = 4\text{ T}$, $\alpha \approx 0.005$, implies anyhow a too large effect on transport properties, which is difficult to reconcile with the change in the band structure for such a relatively small magnetic field. In this respect, we point out that the evidence for a well-defined continuous plot is not so clear for that particular measure of the conductance as in other cases⁴³. More experimental input will be needed, over a complete range of gate voltages, in order to confront the theoretical predictions with a more precise picture of the magnetic field effects on the transport properties.

VII. DISCUSSION

Now we discuss the main distinctive features of our theoretical approach, which lead to very good agreement with the experimental observations.

I) The novelty of our framework reflects itself in the prediction of the periodic dependence of the exponent α on the Fermi energy of the system, due to the oscillatory behavior of the factor $N_T(\varepsilon_F)$ as the Fermi level sweeps the structure of single-particle levels. We estimated the value of $\Delta\varepsilon$ in section II and inferred the variation needed in the gate voltage V_g to produce that shift in energy from the capacitive coupling between the gate and the MWNT. We thus estimated a value of the period for V_g

of the order of $\sim 2\text{ V}$, in agreement with the experimental results. As we have shown in Fig. 7, our model can explain the oscillations in the α exponent, leading to plots that are in good qualitative agreement with the experimental results showing the dependence on the gate voltage. The precise form of these experimental observations may change from one sample to another, but it remains clear that the oscillations with periodicity ΔV_g are in correspondence with the level spacing due to the quantization of single-particle levels.

II) The oscillations in the experimental plot of α vs. V_g were observed for values of $k_B T$ lower than a threshold which is consistent with our estimate for the level spacing $\Delta\varepsilon$. Furthermore, our approach explains naturally the existence of an inflection point T^* in the log-log plot of the conductance versus the temperature, for values of V_g corresponding to peaks in the plot of α . As reported in Ref. 30, the conductance keeps following an approximate power-law behavior below the temperature T^* , but with an exponent significantly enhanced with respect to the high-temperature value. In our model, this is a natural consequence of the asymmetry in the range of variation of α in the upper plot of Fig. 6, when the mean value of the product $N_s N_T$ is in the range 6 – 10. Peak values of α as large as ≈ 0.3 can be reached at low temperatures (which means $N_T < 1$). However, minimum values of α are reached at the other side of the oscillation, for $N_T > 1$. In that case, low temperature does not mean a significant change of the exponent with respect to the mean, high-temperature value.

Thus, it can be shown that our approach provides a sensible description of the power-law dependence and the inflection point in the plot of the conductance as a function of temperature. In our framework, we may introduce the temperature as the relevant variable by trading the scale dependence on the cutoff E_c by scale dependence on the thermal energy $k_B T$. Then we can apply renormalization group equations like (21), but now taking into account that the right-hand-side $\alpha(g)$ depends on temperature through the factor N_T . We have represented in Fig. 10 the behavior of the conductance G that results from the temperature dependence of the renormalization factor $Z(k_B T)$. We observe that an inflection point in the log-log plots appears only for peak values of the α exponent, with values of the crossover temperature T^* corresponding to $k_B T^* \sim \Delta\varepsilon$ ⁴⁵. Our description is also consistent with the experimental fact that such inflection points arise for gate voltages giving the largest values of α . In our approach, the smaller values of α correspond in general to oscillations along the lower curve in Fig. 6, which naturally lends less sensitivity to the exponent upon changes in the temperature variable.

VIII. CONCLUDING REMARKS

In this paper we have developed a framework that applies to an intermediate regime between that of the

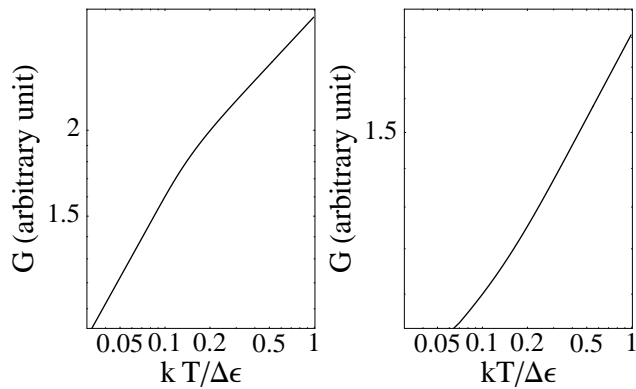


FIG. 10: Log-log plots of the conductance as a function of the temperature. In the left plot the Fermi energy is fixed at $\varepsilon_F \approx 3.7\Delta\varepsilon$, i.e. at the last peak shown in Fig. 7. In the right plot the Fermi energy is fixed at $\varepsilon_F \approx -3.7\Delta\varepsilon$, i.e. at the first minimum shown in Fig. 7.

Coulomb blockade and the Luttinger liquid behavior. Our approach accounts for the main experimental features in the zero-bias conductance reported in Ref. 30. This represents a significant progress with respect to the arguments presented in that reference to interpret the experimental observations. There it was actually claimed that a nonconventional Coulomb blockade, arising from tunneling into a strongly interacting disordered metal, could be at the origin of the exponent oscillations. However, it was also noted that such a theory does not predict power-law behavior above the inflection temperature T^* . The authors of Ref. 30 concluded that “detailed theoretical and experimental investigations would be required for quantitative consideration”.

We believe actually that, regarding transport measurements, the role of disorder is different than that attributed in Ref. 30 to interpret the experimental results. The nonconventional Coulomb blockade predicts a power-law behavior of the conductance, with an exponent given in terms of the mean free path l by $\alpha \approx R/N_s l$. Within this theory, the oscillatory behavior of the exponent was related to the possible modulation of the mean free path coming from disorder. This was supported by recalling the theoretical work of Choi *et al.*³³ about the influence of different forms of disorder on the local density of states. A closer look at this study shows, however, that it is highly unlikely that the combined effect of different defects may produce the desired oscillatory pattern.

From the results of Choi *et al.* in Ref. 33, we note that most part of the impurities and defects of the carbon lattice have an effect on the density of states extending

over an energy range much larger than 1 meV. This is the energy scale consistent with the observed oscillations in the α exponent. Thus, from that source of disorder we can only expect a more or less uniform effect on the range of gate voltage shown in the plots of Fig. 1. On the other hand, the effect of vacancies in the lattice is to produce much narrower peaks in the density of states, which now may give rise to features discernible at the meV scale. We believe that this may be the main origin of the irregularities observed in the oscillations of the α exponent.

Finally, we have also shown that our framework is consistent with the experimental results reported in Ref. 30 about the magnetic field effects in the transport properties. Using a tight-binding approximation adapted to include the action of a transverse magnetic field, we have computed the change in the band structure of the thick shells in multi-walled nanotubes. In this case, the radius of the shells becomes comparable to the magnetic length already for a magnetic field of 4 T. Then, we have seen that the low-energy subbands show an incipient tendency to flatten along Landau levels. This may induce in general further modulation of the exponent α , depending on the strength of the magnetic field.

We have seen that, for high values of α at $B = 0$ (about ≈ 0.3), our approach predicts a sensible reduction of the exponent, which is in agreement with the experimental observation. As long as the density of states at the Fermi level is reduced upon application of the magnetic field, we find a picture that is consistent with the statement that, in most cases, α is smaller for higher magnetic fields³⁰. However, a clarification from the experimental point of view is required, in order to know the exceptions to that rule. In our framework, we may envisage some instances in which the application of the magnetic field may induce the proximity of the Fermi level to the top of a given subband, with the consequent increase in the density of states (and the effective e - e interaction). We find in this way that sufficiently large variations in the magnetic field may produce a modulation in the exponent α , rather than a monotonous trend. Our model provides anyhow definite predictions that are susceptible of being confronted experimentally. In this respect, more experimental input would be desirable to discern the effects of a transverse magnetic field, that may be quite significant for the outer shells in multi-walled nanotubes.

Acknowledgments

J. G. acknowledges the financial support of the Ministerio de Educación y Ciencia (Spain) through grant BFM2003-05317. E. P. was also supported by INFN Grant 10068.

¹ S. Iijima, Nature **354**, 56 (1991).

² P.L. McEuen, Nature **393**, 15 (1998)

- ³ J.W. Mintmire, B.I. Dunlap, C.T. White, Phys. Rev. Lett. **68**, 631 (1992); N. Hamada, S. Sawada, A. Oshiyama, Phys. Rev. Lett. **68**, 1579 (1992); R. Saito, M. Fujita, G. Dresselhaus, M.S. Dresselhaus, Appl. Phys. Lett. **60**, 2204 (1992).
- ⁴ S. Frank, P. Poncharal, Z. L. Wang and W. A. de Heer, Science **280**, 1744 (1998).
- ⁵ A. Urbina, I. Echeverria, A. Perez-Garrido, A. Diaz-Sanchez and J. Abellan, Phys. Rev. Lett. **90**, 106603 (2003).
- ⁶ C. Schönenberger A. Bachtold, C. Strunk and J.P. Salvetat, Appl. Phys. A **69**, 283 (1999)
- ⁷ A. Bachtold, M. de Jonge, K. Grove-Rasmussen, P. L. McEuen, M. Buitelaar and C. Schönenberger, Phys. Rev. Lett. **87**, 166801 (2001).
- ⁸ A. Bachtold et al., Nature (London) **397**, 673 (1999).
- ⁹ A. Kanda et al., Microelectron. Eng. **63**, 33 (2002).
- ¹⁰ N. Kang et al., Phys. Rev. B **66**, 241403 (2002).
- ¹¹ M. Bockrath, D. H. Cobden, P. L. McEuen, N.G. Chopra, A. Zettl, A. Thess and R. E. Smalley, Science **275**, 1922 (1997).
- ¹² S. J. Tans, M. H. Devoret, R. J. A. Groeneveld, C. Dekker, Nature **386**, 474 (1997).
- ¹³ D. H. Cobden and J. Nygard, Phys. Rev. Lett. **89**, 46803 (2002).
- ¹⁴ W. Liang M. Bockrath and H. Park, Phys. Rev. Lett. **88**, 126801 (2002).
- ¹⁵ S. Bellucci and P. Onorato, Phys. Rev. B **71** 075418 (2005).
- ¹⁶ M. R. Buitelaar, A. Bachtold, T. Nussbaumer, M. Iqbal and C. Schönenberger Phys. Rev. Lett. **92**, 156801 (2002).
- ¹⁷ S. Tomonaga, Prog. Theor. Phys. **5**, 544 (1950); J. M. Luttinger, J. Math. Phys. **4**, 1154 (1963); D. C. Mattis and E. H. Lieb, J. Math. Phys. **6**, 304 (1965).
- ¹⁸ V. J. Emery, in *Highly Conducting One-Dimensional Solids*, ed. J. T. Devreese, R. P. Evrard and V. E. Van Doren (Plenum, New York, 1979).
- ¹⁹ J. Solyom, Adv. Phys. **28**, 201 (1979).
- ²⁰ F. D. M. Haldane, J. Phys. C **14**, 2585 (1981).
- ²¹ M. Bockrath, D.H. Cobden, J. Lu, A.G. Rinzler, G. Andrew, R.E. Smalley, L. Balents, P.L. McEuen, Nature **397**, 598 (1999).
- ²² J. Nygard, D.H. Cobden, M. Bockrath, P. L. McEuen, P.E. Lindelof, **69**, 297 (1999).
- ²³ Z. Yao, H.W.J. Postma, L. Balents, C. Dekker, Nature **402**, 273 (1999).
- ²⁴ H.W.C. Postma, M. de Jonge, Z. Yao, C. Dekker, Phys. Rev. B **62**, R10653 (2000); H.W.C. Postma, T. Teepen, Z. Yao, M. Grifoni, C. Dekker, Science **293**, 76 (2001).
- ²⁵ C. L. Kane and M. P. A. Fisher, Phys. Rev. B **46**, 15233 (1992); C. L. Kane and M. P. A. Fisher, Phys. Rev. Lett. **68**, 1220 (1992).
- ²⁶ S. Bellucci and J. González, Eur. Phys. J. B **18**, 3 (2000); S. Bellucci, *Path Integrals from peV to TeV*, eds. R. Casalbuoni, et al. (World Scientific, Singapore, 1999) p.363, hep-th/9810181.
- ²⁷ S. Bellucci and J. González, Phys. Rev. B **64**, 201106(R) (2001).
- ²⁸ S. Bellucci, J. González and P. Onorato, Nucl Phys. B **663** [FS], 605 (2003).
- ²⁹ S. Bellucci, J. González and P. Onorato, Phys. Rev. B **69**, 085404 (2004).
- ³⁰ A. Kanda, K. Tsukagoshi, Y. Aoyagi and Y. Ootuka, Phys. Rev. Lett. **92**, 36801 (2004).
- ³¹ R. Egger, Phys. Rev. Lett. **83**, 5547 (1999)
- ³² R. Egger and A. O. Gogolin, Phys. Rev. Lett. **87**, 066401 (2001).
- ³³ H. J. Choi et al., Phys. Rev. Lett. **84**, 2917 (2000).
- ³⁴ S. Bellucci, J. González and P. Onorato, Phys. Rev. Lett. **95**, 186403 (2005).
- ³⁵ A. Kanda et al., Appl. Phys. Lett. **79**, 1354 (2001).
- ³⁶ C. W. J. Beenakker, Phys. Rev. B **44**, 1646 (1991).
- ³⁷ R. Egger and A. O. Gogolin, Phys. Rev. Lett. **79**, 5082 (1997); Eur. Phys. J. B **3**, 281 (1998).
- ³⁸ C. Kane, L. Balents and M. P. A. Fisher, Phys. Rev. Lett. **79**, 5086 (1997).
- ³⁹ R. Egger, H. Grabert, Phys. Rev. Lett. **79**, 3463 (1997) .
- ⁴⁰ For the dominant forward-scattering processes considered here, a sensible average of the interaction is given by $q_0 \sim 1/L$.
- ⁴¹ M. Krüger, M.R. Buitelaar, T. Nussbaumer, C. Schönenberger, L. Forró, Appl. Phys. Lett. **78**, 1291 (2001).
- ⁴² R. Saito, G. Dresselhaus and M. S. Dresselhaus, *Physical Properties of Carbon Nanotubes*, Chap. 6, Imperial College Press, London (1998).
- ⁴³ One cannot discard however a nontrivial interplay between the quantum Hall regime and the Luttinger liquid regime at large magnetic fields. Perturbative evidence of that has been provided for instance in Refs.⁴⁴.
- ⁴⁴ S. Bellucci and P. Onorato, *Magnetic field effects and renormalization of the long-range Coulomb interaction in Carbon Nanotubes*, accepted for publication in Annals of Physics (2005), cond-mat/0510590; S. Bellucci and P. Onorato, European Physical Journal B **45**, 87 (2005).
- ⁴⁵ The form of the crossover is here slightly different to that in the plot provided in Ref.³⁴. This comes from the use there of a rough approximation for the conductance, $G \sim T^\alpha$, with the T -dependent exponent α . The differential renormalization given by Eq. (21) provides however a more accurate description of the crossover, leading to the plot shown to the left in Fig. 10.